




# Heterotrophic Bacteria Dominate the Diazotrophic Community in the Eastern Indian Ocean (EIO) during Pre-Southwest Monsoon

Chao Wu<sup>1</sup> · Jinjun Kan<sup>2</sup> · Haijiao Liu<sup>1</sup> · Laxman Pujari<sup>3,4</sup> · Congcong Guo<sup>3,4</sup> · Xingzhou Wang<sup>3,4</sup> · Jun Sun<sup>3,4,5</sup> 

Received: 12 June 2018 / Accepted: 5 March 2019 / Published online: 29 April 2019  
© Springer Science+Business Media, LLC, part of Springer Nature 2019

## Abstract

The diazotrophic communities play an important role in sustaining primary productivity through adding new nitrogen to oligotrophic marine ecosystems. Yet, their composition in the oligotrophic Indian Ocean is poorly understood. Here, we report the first observation of phylogenetic diversity and distribution of diazotrophs in the Eastern Indian Ocean (EIO) surface water (to 200 m) during the pre-southwest monsoon period. Through high throughput sequencing of *nifH* genes, we identified diverse groups of diazotrophs in the EIO including both non-cyanobacterial and cyanobacterial phylotypes. Proteobacteria (mainly Alpha-, Beta-, and Gamma-proteobacteria) were the most diverse and abundant groups within all the diazotrophs, which accounted for more than 86.9% of the total sequences. Cyanobacteria were also retrieved, and they were dominated by the filamentous non-heterocystous cyanobacteria *Trichodesmium* spp. Other cyanobacteria such as unicellular diazotrophic cyanobacteria were detected sporadically. Interestingly, our qPCR analysis demonstrated that the depth-integrated gene abundances of the diazotrophic communities exhibited spatial heterogeneity with *Trichodesmium* spp. appeared to be more abundant in the Bay of Bengal ( $p < 0.05$ ), while *Sagittula castanea* (Alphaproteobacteria) was found to be more dominating in the equatorial region and offshores ( $p < 0.05$ ). Non-metric multidimensional scaling analysis (NMDS) further confirmed distinct vertical and horizontal spatial variations in the EIO. Canonical correspondence analysis (CCA) indicated that temperature, salinity, and phosphate were the major environmental factors driving the distribution of the diazotroph communities. Overall, our study provides the first insight into the diversity and distribution of the diazotrophic communities in EIO. The findings from this study highlight distinct contributions of both non-cyanobacteria and cyanobacteria to N<sub>2</sub> fixation. Moreover, our study reveals information that is critical for understanding spatial heterogeneity and distribution of diazotrophs, and their vital roles in nitrogen and carbon cycling.

**Keywords** Diazotroph · Heterotrophic bacteria · *Trichodesmium* · High throughput sequencing · Nitrogen fixation · The eastern Indian Ocean

## Introduction

Biological nitrogen fixation (BNF), the enzyme-catalyzed reduction of dinitrogen (N<sub>2</sub>) from air to bioavailable ammonium, is

identified a major source of nitrogen in N-starving marine ecosystems [1, 2]. Multiple studies have highlighted the significance of N<sub>2</sub> fixation in sustaining marine primary production, powering the biological carbon pump, and eventually accelerating carbon

**Electronic supplementary material** The online version of this article (<https://doi.org/10.1007/s00248-019-01355-1>) contains supplementary material, which is available to authorized users.

✉ Jun Sun  
phytoplankton@163.com

<sup>1</sup> Institute of Marine Science and Technology, Shandong University, Qingdao 266237, China

<sup>2</sup> Microbiology Division, Stroud Water Research Center, Avondale, PA 19311, USA

<sup>3</sup> Tianjin Key Laboratory of Marine Resources and Chemistry, Tianjin University of Science and Technology, Tianjin 300457, China

<sup>4</sup> Research Centre for Indian Ocean Ecosystem, Tianjin University of science and Technology, Tianjin 300457, China

<sup>5</sup> College of Marine & Environmental Sciences, Tianjin University of Science and Technology, No.29 13th Avenue, TEDA, Tianjin 300457, People's Republic of China

sequestration to the ocean [3–5]. Based on in situ experiments, the fixed nitrogen by the diazotrophic communities was estimated to fuel up to half or more of primary production in the subtropical North Pacific and tropical North Atlantic regions [6, 7]. BNF is a process catalyzed by a nitrogenase enzyme complex in a selected group of microorganisms termed as diazotrophs. Nitrogenase is a highly conserved enzyme which consists of two multisubunit metallo-proteins, namely, dinitrogenase reductase and dinitrogenase encoded by *nifH* and *nifKD* [8]. Due to its highly conserved sequences, *nifH* gene has been widely used for phylogenetic and ecological studies of the diazotrophic communities in marine ecosystems [9].

The molecular techniques have revolutionized the traditional method of identifying  $N_2$  fixers via a microscope, and a wide range of diazotrophs have been separated and identified from marine environments [10]. Ever since, related studies of diazotrophs on biogeochemical, physio-ecological, and molecular aspects have been thriving and prosperous. Among all the diazotrophic communities, Proteobacteria and cyanobacteria are identified as the most abundant groups inhabiting euphotic layer of marine ecosystems [11]. Cyanobacteria have a broad geographic distribution and contain a variety of morphologic and phylogenetic groups including *Trichodesmium* spp., diatom-diazotroph symbioses, and unicellular  $N_2$  fixing cyanobacteria (groups A, B, and C) [12]. Previous studies have been mainly focused on cyanobacterial diazotrophs which are widely distributed in tropical and subtropical oceans. More recently, Proteobacteria, including Alpha-, Beta-, Gamma-, and Delta-proteobacteria, were reported dominant in open oceans such as the northern South China Sea, the Southern Indian Ocean, and the Eastern Tropical South Pacific region [13–15]. The dominance of Proteobacteria in open oceans reveals that our understanding of the diazotrophic community is still limited. Further studies focusing on physiological and ecological characterizations of these widely distributed bacteria and their interactions with environmental gradients have important implications for understanding their contribution to nitrogen fixation and global nitrogen cycling [16].

As the third largest ocean in the world, the Indian Ocean plays a significant role in global climatic change, energy flow, and material cycles [17]. The Indian Ocean is divided into two semi-enclosed basins in the north by Indian subcontinent and extends to at least 26°N in the south. North Indian Ocean is heavily influenced by the South Asian monsoon system. The surface circulation changes seasonally in response to the prevalent monsoons, with Somali Current flowing equatorward during the winter monsoon and poleward during summer monsoon [18, 19]. Upwelling and convective mixing induced by seasonally reversing monsoon winds can increase upward supply of nutrients and cause algal blooms seasonally in the northern Indian Ocean [20, 21]. It is generally believed that

the Bay of Bengal (BOB) is less productive than the Arabian Sea (AS), partly due to the freshwater input which decrease the salinity on the surface and aggravate stratification [20, 22–24]. Winds over the northern Indian Ocean are generally weak during the period of pre-southwest monsoon, and stratified water results in low supplement of the nutrient from deeper water. Strong stratification, calm water, sufficient solar heating, and extreme oligotrophic condition make the northern Indian Ocean an ideal habitat for the diazotroph community during the pre-southwest monsoon period. In fact, surface blooms of *Trichodesmium* spp. are well documented in both the AS and the BOB [25–27], and heterotrophic bacteria have been reported dominant among diazotrophs in the AS during the winter monsoon [14, 28]. However, no detailed studies have been conducted in investigating composition and distribution of the diazotrophic communities at the BOB and the eastern Equator region.

Compared to the North Pacific [29–31] and North Atlantic [32–35], the diazotrophic community in Indian Ocean is understudied, and currently available data are primarily focused on the AS [14, 28]. In the present study, we collected water samples in the BOB and the open region of eastern equatorial Indian Ocean during the pre-southwest monsoon of 2017. In order to investigate composition and spatial distribution of the diazotrophic communities in the EIO, molecular approaches including high throughput sequencing analysis and real-time fluorescent quantitative polymerase chain reaction (qPCR) assay were applied to samples collected from different locations and depths. The high throughput sequencing analysis provided detailed information of the diazotrophic community structures including dominant and rare species, as well as uncultured populations. Based on the results of high throughput sequencing, qPCR assay was used to quantify the dominant diazotrophic groups in the EIO. In addition, multivariate statistics were conducted between communities and environmental parameters to determine the controlling factors in structuring diazotrophs.

## Materials and Methods

### Station Location, Sampling, and Physicochemical Analysis

The cruise was carried out in the EIO onboard R/V “Shiyan 3” from 9 March to 7 April 2017. Samples for molecular analyses were collected from 10 sampling sites at seven depths (0 m, 25 m, 50 m, 75 m, 100 m, 150 m, and 200 m) for each site. The sampling sites were located along four main transects targeting the BOB (I1, I2), the Equator region (I4), and the transect (I5) parallel to the coastline of the Sumatra (Fig. 1). Among all the stations, we chose six

stations (I105, I504, I203, I210, I405, and I413) with three depths (0 m, 75 m, and 200 m) for high throughput sequencing (Fig. 1). Whereas for qPCR analysis, all samples were included (10 stations and 7 depths as shown in Fig. 1 and Table 1). Surface water was collected by using 10% HCl-rinsed polyethylene (PE) bucket at all the stations. Vertical seawater was collected by using 5 L Teflon-coated Go-Flo bottles (General Oceanics, Miami, Florida, USA) attached to a rosette multisampler, on which conductivity, temperature, and depth (CTD) probes were installed (Seabird SBE 911Plus, Sea-Bird Electronics, Washington, USA). Temperature and salinity were measured and recorded vertically by a CTD profiler.

### Sample Collection and Environmental Parameter Measurements

Water samples from different layers were transferred individually into 15 L PE buckets that were previously washed with 10% HCl and rinsed thrice with Milli-Q water. Samples for determination of nutrients were subsampled into 100 mL of 10% HCl-rinsed PE bottles and stored in 4 °C until analysis. In the laboratory, nutrient concentrations including ammonium ( $\text{NH}_4^+$ ), nitrate ( $\text{NO}_3^-$ ), nitrite ( $\text{NO}_2^-$ ), phosphate ( $\text{PO}_4^{3-}$ ), and silicate ( $\text{SiO}_3^{2-}$ ) were determined by using a Technicon AA3 Auto-Analyzer (Bran+ Luebbe, Norderstedt, Germany) based on the classical colorimetric methods [36]:  $\text{NH}_4^+$ , dissolved

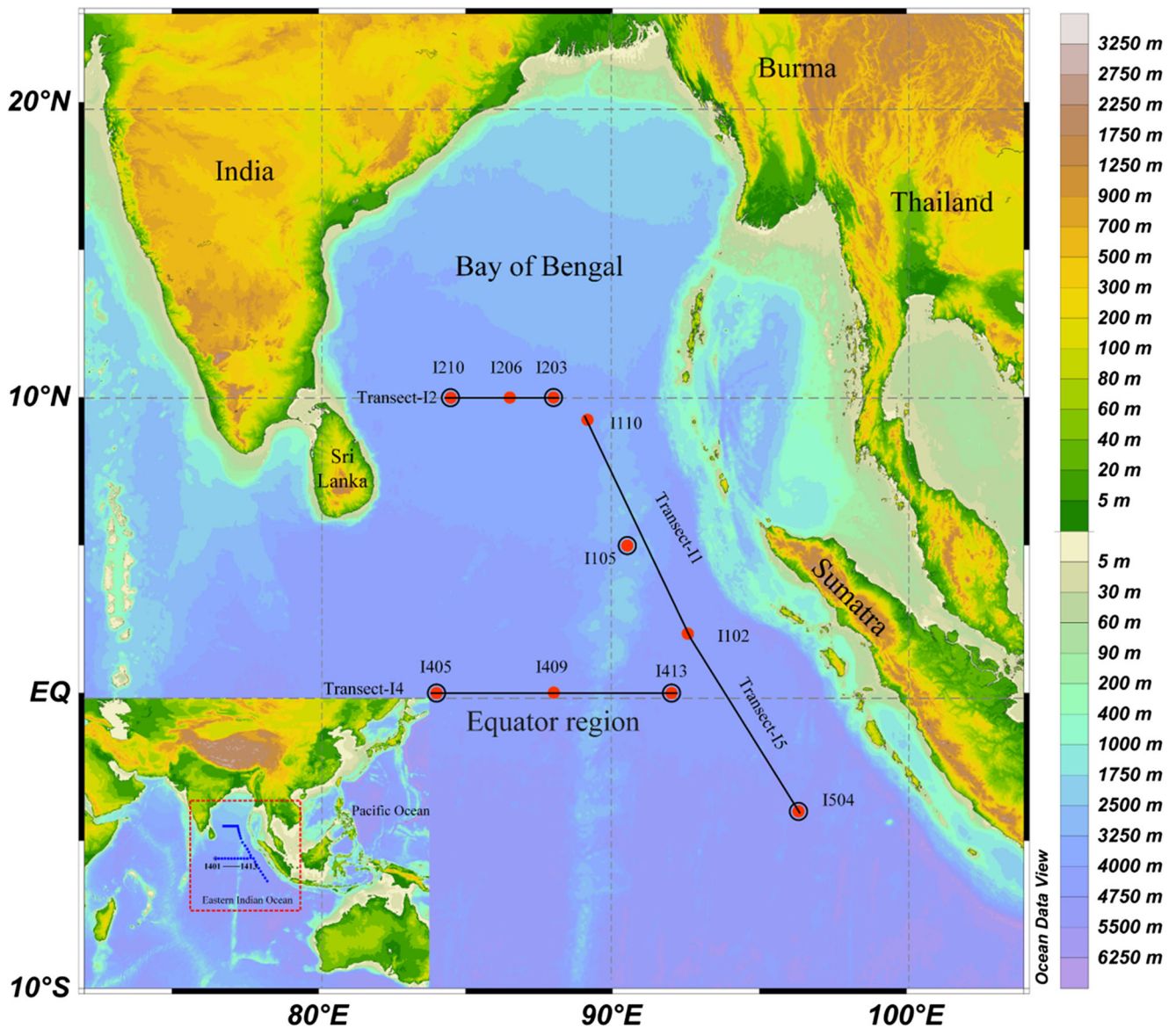


**Fig. 1** The map showing the sampling stations in the EIO. Miniature map at lower left described the transects and stations for hydrography measurement (blue dots in red box). In enlarged map of the EIO, 10

sites (red dots) were used for qPCR analysis and 6 sites (circled) were subjected to high throughput sequencing

**Table 1** Temperature (T), salinity (S), chlorophyll *a* (Chl *a*) concentration, and dissolved inorganic nutrients (ammonium, nitrate, nitrite, phosphate) in surface water at sampling stations

Station	Data	Longitude (E)	Latitude (N or S)	Depth (m)	T (°C)	Salinity	Chl <i>a</i> (µg L <sup>-1</sup> )	NO <sub>3</sub> <sup>-</sup> (µM)	NO <sub>2</sub> <sup>-</sup> (µM)	NH <sub>4</sub> <sup>+</sup> (µM)	PO <sub>4</sub> <sup>3-</sup> (µM)
I102	2017-3-13	92°34'9"	1°59'52"	4361	29.4	32.1	0.081	0.429	0.143	0.714	0.100
I105	2017-3-15	90°30'10"	4°59'34"	3338	29.5	34.1	0.103	0.421	0.257	0.207	0.090
I110	2017-4-7	89°8'2"	9°14'45"	3443	30.3	31.0	0.085	0.393	0.221	0.586	0.065
I203	2017-4-7	87°59'39"	10°0'1"	3421	30.3	32.9	0.341	0.950	0.200	1.371	0.100
I206	2017-4-5	86°29'50"	9°59'51"	3513	31.1	32.7	0.295	0.157	0.214	1.007	0
I210	2017-4-4	84°29'38"	9°59'36"	3575	30.0	33.2	0.126	0.379	0.157	1.071	0.035
I405	2017-3-19	83°59'54"	0°0'6"	4548	29.7	33.8	0.067	0	0.129	0.443	0.126
I409	2017-3-18	88°0'5"	0°0'14"	4507	29.3	33.5	0.101	2.043	0.200	1.300	0.145
I413	2017-3-12	92°0'8"	0°0'8"	5422	29.4	32.5	0.100	0.679	0.143	1.379	0.126
I504	2017-3-9	96°20'4"	3°59'53"	5095	29.5	33.5	0.076	0.129	0.136	0.757	0.061

inorganic nitrogen (DIN), PO<sub>4</sub><sup>3-</sup>, and SiO<sub>3</sub><sup>2-</sup> are measured by indophenol blue method, the copper-cadmium column reduction methods, phosphor-molybdate complex methods, and silico-molybdate complex methods, respectively.

For Chl *a* analysis, 500 mL water from each layer were vacuum-filtered (< 10 mmHg) through a 25-mm GF/F filter (Waterman, Florham Park, NJ, USA). The filters were placed into aluminum foil bags and stored in the dark at -20 °C until analyzed. In the lab, filters were kept in 20 mL vials and pigments were extracted with 90% acetone (Guanghui, Yixing, Jiangsu, China) for 24 h at 4 °C. Chlorophyll concentrations were then determined using a Turner® Trilogy (CHL NA, model no. 046) fluorometer (Turner designs, San Jose, CA, USA). For molecular analyses, 2–4 L of seawater were filtered through 0.22-µm GTTP filters (Millipore, Eschborn, Germany) under low pressure vacuum. The filters were placed into 2-mL microtubes, and flash frozen immediately in liquid nitrogen on board. The filters were transferred to -80 °C freezer in the lab until DNA extraction.

### DNA Extraction, *nifH* Gene Amplification, and Sequencing

Genomic DNA were extracted by CTAB method as previously described with minor modifications [37, 38]. Briefly, filters were cut into small pieces and placed into 1.5-mL sterile centrifuge tubes. For each extraction, 600-µL CTAB extraction buffer and 15 µL 2% β-mercaptoethanol (Goabio, Beijing, China) were added and incubated at 60 °C in a water bath for 60 min. Proteins, polysaccharides, and other impurities were separated by adding equal volume of 24:1 chloroform:isoamyl alcohol (Solarbio, Beijing, China), and then centrifuged at 14000 rpm for 20 min at 4 °C. Supernatant was transferred into a new clean tube, and this step was repeated once to insure complete removal of impurities. The genomic DNA were precipitated overnight at -20 °C by addition of 2/3 volume of

isopropanol (Sangon Biotech, Shanghai, China) followed by washing with 75% ethanol (Hushi, Shanghai, China) twice, then air-dried genomic DNA pellet was eluted with 70 µL sterile ultra-pure water and stored at -20 °C until further processing. Note that the solutions used in our experiment were all marked with molecular grade. The quantity and quality of genomic DNA were checked by using a ND-2000 Nanodrop spectrometer (Thermo Fisher Scientific, Wilmington, Delaware, USA).

The *nifH* gene fragments were amplified from the genomic DNA through nested polymerase chain reaction (nested PCR) according to a previous protocol [10]. PCRs were performed using a Veriti 9902 thermocycler (Applied Biosystems, Foster City, CA, USA) with 10 µL reaction volumes containing 1× PCR buffer, 4 mM MgCl<sub>2</sub>, 400 mM dNTPs, 1 µM forward, and reverse primers (*nifH3* and *nifH4* for primary, *nifH1* and *nifH2* for secondary PCR), 0.2-unit KOD FX Neo polymerase (Toyobo, Osaka, Japan), and 1 µL of template DNA (genomic DNA for the first round, and PCR products from the primary PCR for the second round). Negative controls were set up by replacing template DNA with nuclease-free water. The thermal profile used for the *nifH* gene amplification was initial denaturation (95 °C, 5 min), followed by 38 (primary) or 40 (secondary) cycles of denaturation (94 °C, 1 min), annealing (52 °C for the first round and 59 °C for the second round, 1 min), and extension (72 °C, 1 min) with a final extension (72 °C, 7 min). Remarkably, primers used in secondary PCR were composed of dual-indexed barcodes, Illumina linkers, a sequencing primer binding region, and gene-specific sites. PCR products were checked by 1.8% agarose gel (BioWest, Castropol, Spain) electrophoresis after amplification, and products with approximately 360 bp bands were used for high throughput sequencing. All libraries were constructed and sequenced via paired-end chemistry (PE250) on an Illumina Hiseq2500 platform (Illumina, San Diego, CA, USA) at Biomarker Technologies, Beijing, China.

## Quality Control and Sequencing Data Processing

The raw image data file obtained from Illumina HiSeq2500 platform were transformed into sequenced reads via base calling, and the results were stored in the format of FASTQ file which include the information of raw sequence data and corresponding sequencing quality. The raw sequence data were then separated by samples based on their barcodes, permitting up to one mismatch [39]. The raw sequence data were demultiplexed, quality filtered, and analyzed through the open-source software pipeline QIIME [40], and the paired reads were merged into full-length sequences by FLASH v1.2.7 software [41]. For each sample, the raw tags were quality filtered to get high-quality clean tags via Trimmomatic v0.33 software [42], including removal of sequences less than 300 bases, homopolymers containing sequences (homopolymers  $\geq 8$  bases), and ambiguous base containing sequences [43, 44]. The barcodes, linker sequences, and primers were also removed in this process. Effective tags were subsequently obtained after removing chimera by UCHIME v4.2 software [45]. The remaining effective tags were clustered using USEARCH v10.0 at 97% similarity to generate operational taxonomic units (OTUs) [46]. Low abundance OTUs which containing less than 20 sequences across all samples were excluded from further processing.

To identify dominant taxa, top OTUs in each sample were selected for subsequent phylogenetic analysis. The most common sequences in each OTU were selected as the representative sequences. These sequences were first translated into amino acid sequences and blasted in the protein database at National Center for Biotechnology Information (NCBI) via BLASTX v2.8.1+ to identify the most closely related sequences [47]. The representative sequences and the most closely related sequences were then aligned with ClustalW and used to construct a phylogenetic neighbor-joining tree by MEGA v7.0 [48, 49]. Cluster stability was tested by bootstrap resampling for 1000 times, and the phylogenetic tree was further edited by an online webpage iTOL [50]. The raw sequences obtained from this study were deposited in NCBI Sequence Read Archive with accession no. SUB3781024.

## Quantification of Two Cyanobacterial and Two Non-Cyanobacterial *nifH* Phylotypes

According to the results of high throughput sequencing, abundance of four top diazotrophs, namely, *Trichodesmium* spp., *Crocospaera watsonii*, *Sagittula castanea*, and  $\gamma$ -24774A11, were quantified by qPCR using an ABI Step One Plus Real-Time PCR System (Applied Biosystems, Foster City, CA, USA). The specific primers and probes shown in Table 2 were designed by previous studies with minor modifications to correct mismatch [33, 51]. The specificity of the primers and probes were all checked in the abovementioned studies, and no significant cross-reactivity was observed. The TaqMan probes were 5'-labeled with the fluorescent reporter FAM (6-carboxyfluorescein) and 3'-labeled with the quenching dye TAMRA (6-carboxytetramethylrhodamine). All primers and probes used in the present study were synthesized in Sangon Biotech, Shanghai, China. For all TaqMan PCRs, duplicate or triplicate 10  $\mu$ L reactions were performed with 5  $\mu$ L of 2  $\times$  Premix Ex Taq<sup>TM</sup> (Takara Bio, Tokyo, Japan), 0.2  $\mu$ M of the forward and reverse primers, 0.4  $\mu$ M of TaqMan probe, 0.2  $\mu$ L of 50  $\times$  ROX reference dye, 1  $\mu$ L of template DNA, and 3  $\mu$ L of nuclease-free water. The PCR conditions were 95  $^{\circ}$ C for 30 s, followed by 45 cycles of 95  $^{\circ}$ C for 5 s and 60  $^{\circ}$ C for 30 s. Standard curves were determined by analyzing 10-fold serial dilutions of the target *nifH* gene inserted plasmids with a final gene copy numbers ranged from  $10^1$  to  $10^7$  for each reaction. The  $r^2$  values of each standard curve ranged between 0.98 to 1.00, and PCR amplification efficiency ranged from 90 to 110%. The copy numbers of each diazotroph in the environmental samples were calculated based on mean Ct values. Furthermore, non-target templates were also tested in the same conditions, and gene copies in negative controls less than 10 or undetectable were considered contamination-free. The detection limit of qPCR reactions was approximately 50 *nifH* genes in 1- $\mu$ L template DNA, which was equivalent to approximately 3500 copies with a final volume of 70  $\mu$ L in the present study.

**Table 2** Primers and probes used for TaqMan-qPCR analysis targeting two cyanobacterial and two non-cyanobacterial *nifH* phylotypes

Targets	Forward primer (5'-3')	Probe	Reverse primer (5'-3')	Reference
<i>Trichodesmium</i> spp.	GACGAAGTATTGA AGCCAGGTTTC	CATTAAGTGTGTTGAA TCTGGTGGTCTCTGAGC	CGGCCAGCGCAACCTA	Goebel et al. (2010)
<i>Crocospaera watsonii</i>	TGGTCTGAGC CTGGAGTTG	TGTGCTGGTCTGTTGAT	TCTTCTAGGAAGTT GATGGAGGTGAT	Goebel et al. (2010)
<i>Sagittula castanea</i>	ATCACCGCCAT CAACTTCCT	CGCCTACGATGACG TGGATTACGTGTCC	AGACCACGTC GCCAGAAC	Zhang et al. (2011)
$\gamma$ -24774A11	TCCACACGTCTT ATTCTGCACT	AAGTGCTTAAGGTTG GCTTTGGCGACA	AGAGCAAACAAT GTAGATTTCTCTG	Moisander et al. (2014)

## Statistical Analysis

Richness and diversity indices including Chao1 richness estimator, Ace richness estimator, Shannon diversity indices, and Simpson diversity index were calculated with R v 3.3.2 software [52]. To evaluate the coverage of sequencing, the abundance data was standardized and calculated based on entropy (Q statistics) in the online software iNEXT [53, 54]. Rarefaction curves were also done in this online software based on the standard operating procedure shown in the website (<https://chao.shinyapps.io/iNEXTOnline/>). Non-metric multidimensional scaling (NMDS) analysis and cluster analysis were used in the present study to demonstrate vertical and horizontal distribution patterns of the diazotrophic communities in PRIMER V6.0 software [55]. The diazotroph community data was first square-root transformed in the software, and then, a lower triangular resemblance matrix was created based on Bray–Curtis similarity. Subsequently, a hierarchical cluster tree and a NMDS biplot were constructed in the software based on the matrix. To reveal the correlations between the diazotrophic communities and environmental factors, detrended correspondence analysis (DCA) was first carried out by *decorana* function in *vegan* to determine whether redundancy analysis (RDA) or canonical correspondence analysis (CCA) was more suitable [56, 57]. Because the length of gradient value of the first axis was greater than 3.0, CCA was selected to explore correlations between community structure and environmental gradients and run in R v 3.3.2 software. Highly correlated environmental factors were removed by co-linearity test conducted with *vif.cca* function in *vegan* and variance inflation factors (VIFs) of remaining environmental factors were all less than 20 [58]. Depth-integrated (0–200 m) gene abundances were calculated by trapezoidal integration over depths of the euphotic zone, and the results were plotted by ODV V5.0.0 [59]. The significant differences of depth-integrated gene abundances (log-transformed) for diazotrophs among different regions were evaluated by *t* test in IBM SPSS Statistics 25.

## Results

### Hydrography and Environmental Parameters

The surface hydrographic characteristics for all stations were shown in Table 1 and Table S1. During the study period, sea surface temperature (SST) varied from 28.5 to 31.1°C, and BOB had higher SST than other regions ( $p < 0.01$ ). Sea surface salinity (SSS) ranged from 30.4 to 34.3, and BOB had higher SSS than other regions ( $p < 0.05$ ). The maximum and minimum value of SSS was 34.3 ppt at Sta. I404 and 30.4 ppt at Sta. I201, respectively. The surface regime could be distinguished by *T-S* properties

of the upper 200 m at sampling stations where lower salinity and slightly higher temperature were observed at the BOB stations (Fig. 2). The potential density ( $\sigma_0$ ) was less than 21.0  $\text{kg m}^{-3}$  at near surface water at Sta. I110, I203, I206, and I210, followed by nearly 21.0  $\text{kg m}^{-3}$  at other stations except for some unstable data. Chl *a* concentrations ranged from 0.067 to 0.407  $\mu\text{g L}^{-1}$ , and there was no significant difference of surface Chl *a* concentrations in the area study. Across all the sampling stations, concentrations for dissolved inorganic nutrients were quite low in the study area, suggesting the EIO was a typical oligotrophic ocean. For instance, nitrate, nitrite, ammonium, and phosphate concentration ranged from 0 to 2.043  $\mu\text{M}$ , 0.129 to 0.257  $\mu\text{M}$ , 0 to 1.379  $\mu\text{M}$ , and 0 to 0.155  $\mu\text{M}$ , respectively (Table S1).

Vertical profiles of temperature, salinity, dissolved inorganic nutrients, and Chl *a* are shown in Fig. 3 and Fig. S1. The study region was characterized by stable surface waters with higher temperature and lower salinity than deep waters. Obviously, the thermocline and halocline in the Equator region was shallower than other areas and increased gradually from the open oceans to the offshore region. The halocline was clearly observed at the BOB and the Equator region, but not obvious in the offshore section. Vertical profiles of nitrate and phosphate in survey stations showed consistent patterns with lower concentrations in the top 50 m and increased dramatically in deep waters. Nitrite concentrations peaked at 75 m but remained nearly the same in other layers. The Chl *a* maximum layer was at 75 m except for Stn. I105 (50 m instead), and integrated Chl *a* concentrations for top 200 m

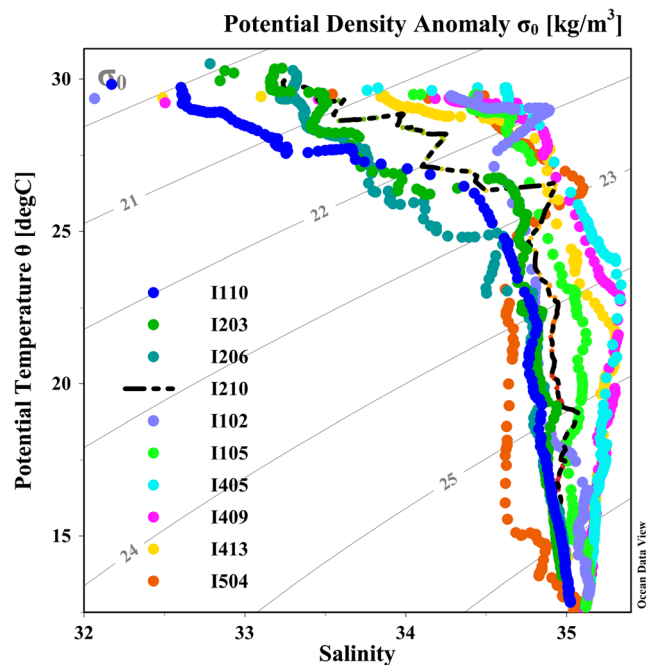


**Fig. 2** Potential temperature ( $\theta$ ) versus salinity scatters (*T-S* properties) in the upper 200 m water column in the EIO

water column ranged from  $27.83 \mu\text{g L}^{-1}$  (Stn. I409) to  $40.70 \mu\text{g L}^{-1}$  (Stn. I105). Compared to other nutrients, no consistent patterns were observed for vertical distribution of ammonium.

### Sequencing Statistics and Diversity Estimates

In total, 1,185,461 effective tags were included in our study after quality control, and the detailed information for each sample was listed in Table 3. The sequencing coverage (C) was all greater than 99.9%, suggesting the sequencing effort was deep enough to cover *nifH* gene diversity. On average, 65,859 sequences per sample were obtained with an average length at 320 bp. Based on 97% similarity, a total of 218 OTUs were obtained after excluding rare OTUs (<20 sequences across all samples). The rarefaction curve plateau are shown in Fig. S2. The OTU richness ranged from 17 to 72, and the minimum and maximum OTUs were observed at Stn. I405 (200 m) and Stn. I210 (75 m), respectively. Combined all alpha diversity indices, the lowest and highest diversities occurred at the same station Stn. I203 but at different layers, 0 m and 75 m, respectively. Overall, Stn. I210 had the highest diversity indices ( $H = 2.39$ ,  $D = 0.86$ ) while the lowest indices occurred in Stn. I405 ( $H = 1.28$ ,  $D = 0.63$ ).

### Phylogeny and Composition of Diazotrophs

Due to large numbers of OTUs recovered and most of them were unidentifiable, we only focused on the top OTUs in the present study. The OTUs contained  $\geq 500$  sequences across all the samples were defined as top OTUs in our study. Top 30 OTUs accounted for more than 97% of all the sequences, and they were included in subsequent phylogenetic analysis (Fig. 4). Reference sequences from NCBI were all retrieved from marine environments, and the unknown species were labeled with ocean names

where they originated. Top 30 OTUs were grouped into three defined clusters of *nifH* genes [2], in which 28 OTUs belonged to cluster I, 1 OTU (*Phasecolarcto bacterium*) belonged to cluster II, and 1 OTU (*Verrucomicrobiae bacterium*) belonged to cluster III (Fig. 4). Nearly half of the OTUs were closely related to Alphaproteobacteria (14/30 OTUs), followed by Betaproteobacteria (5/30 OTUs), Gammaproteobacteria (5/30 OTUs), and Cyanobacteria (4/30 OTUs).

Relative abundance of diazotrophs is shown in Figs. 4 and 5. Overall, Proteobacteria was clearly the most dominant group in the EIO, followed by Cyanobacteria. Within all the diazotrophic community, OTU 550 shared 100% similarity with a recently isolated *Sagittula* (*Rhodobacteraceae*, Alphaproteobacteria) [60] and dominated diazotrophs across all samples. OTU 550 was detected in all the samples but was more abundant in the Equator region (Stn. I405 and I413) and deep layers (Fig. 4). Besides OTU 550, other Alphaproteobacteria such as OTU 115 (*Novosphingobium malaysiense*), OTU 881, and OTU 537 (*Bradyrhizobium* sp.) were also commonly detected. OTU 702 was the second most dominant diazotroph which shared 100% similarity with an uncultured Betaproteobacterium, and its occurrence was noted in deep waters. OTU 536, closely related to Gammaproteobacterium  $\gamma$ -24774A11, was also recovered in the present study though in low abundance. Apart from  $\gamma$ -24774A11, other Gammaproteobacteria including OTU 1136, OTU 1128 (*Vibrio diazotrophicus*), OTU 659, and OTU 388 (*Pseudomonas stutzeri*) were also detected.

In addition, four OTUs were clustered with cyanobacteria, including OTU 229 (*Trichodesmium* spp.), OTU 325 (*Crocospaera watsonii*), OTU 888 (UCYN-A3) and OTU 301 (*Cyanothece* sp. WH 8904). Among which, *Trichodesmium* spp. was the most abundant cyanobacteria, while the other cyanobacteria exhibited low abundances (Fig. 4). *Trichodesmium* sequences were recovered from all

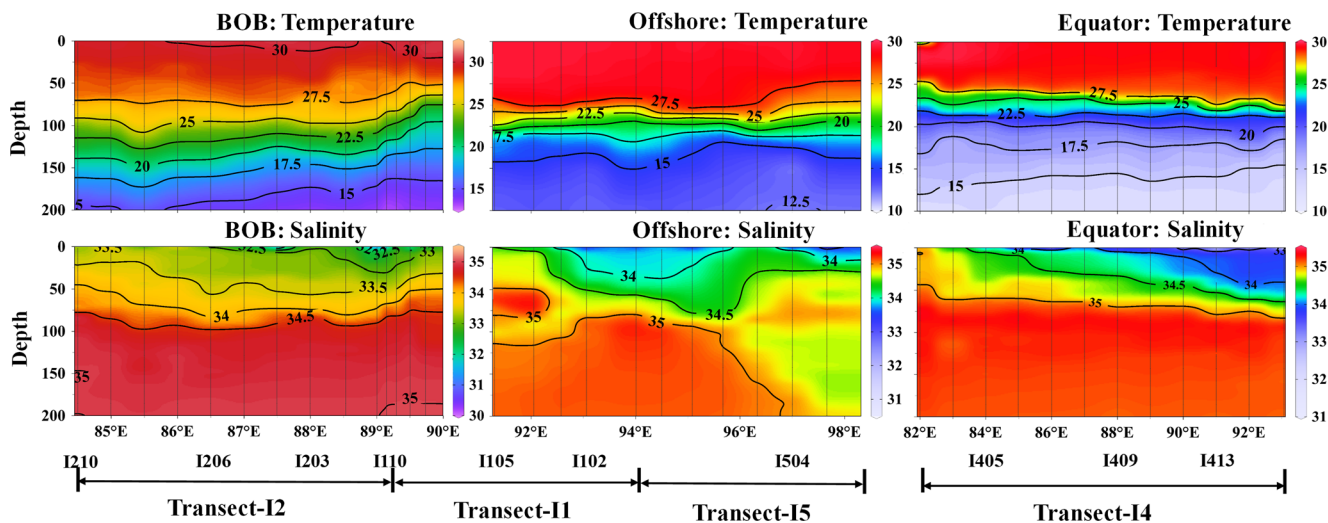


Fig. 3 Depth profiles of temperature and salinity in the BOB (I1, I2), the Equator region (I4), and the transect (I5) parallel to the coastline of the Sumatra

**Table 3** Diversity and predicted richness of *nifH* genes recovered from the EIO by Illumina Hiseq2500 platform

Sites		I105	I504	I203	I210	I405	I413
Surface (0 m)	Effective tags	64,921	64,928	66,946	65,247	66,103	65,990
	No. of OTUs	53	50	26	37	39	58
	Coverage (C%)	99.99	99.98	99.99	99.99	99.99	99.98
	Chao1	61.2	57.9	28	65	43.7	77.5
	Shannon–Weiner (H)	1.40	1.22	0.43	1.76	0.77	1.86
	Simpson (D)	0.58	0.51	0.17	0.75	0.47	0.78
DCM (75 m)	Effective tags	67,185	65,694	65,239	65,241	66,034	64,969
	No. of OTUs	64	50	68	72	36	58
	Coverage (C%)	99.98	99.98	99.99	99.98	100	99.98
	Chao1	80.5	72	71.3	81.2	36.3	70.3
	Shannon–Weiner (H)	1.41	1.22	2.12	1.80	1.36	1.77
	Simpson (D)	0.56	0.63	0.84	0.74	0.66	0.80
Bottom (200 m)	Effective tags	65,479	69,612	67,090	65,335	63,757	65,691
	No. of OTUs	52	67	55	66	19	66
	Coverage (C%)	99.98	99.99	99.99	99.98	99.99	99.99
	Chao1	74	82	60.6	79	20.8	66.6
	Shannon–Weiner (H)	1.22	1.25	1.39	1.41	0.75	1.40
	Simpson (D)	0.62	0.47	0.68	0.59	0.51	0.68

surface waters except for Stn. I405. Compared to the Equator area, *Trichodesmium* was more abundant at the BOB, especially at Stn. I203 where *Trichodesmium* blooms might have occurred. Meanwhile, *Crocospaera watsonii*, UCYN-A3, and *Cyanothece* sp. WH 8904 were mainly detected in surface waters at Stn. I210 and I413.

### Quantification of Dominant *nifH* Phylotypes

Abundances for four major *nifH* phylotypes (*Sagittula castanea*,  $\gamma$ -24774A11, *Trichodesmium* spp. and UCYN-B) were quantified by qPCR. The Ct values of non-target template were all undiscovered or in high values for *Sagittula castanea* (not detected),  $\gamma$ -24774A11 (Ct = 38), *Trichodesmium* (not detected), and UCYN-B (Ct = 35.4). The sensitivity and accuracy of standard curves for different targets were shown in Table 4.

Depth profiles of *nifH* genes for the four dominant phylotypes are shown in Fig. 5, and the depth-integrated abundances (up to 200 m) were shown in Fig. 6. The highest abundances were usually detected in the upper layer from 0 to 50 m. *Sagittula castanea* was detected at all stations with all depths, and peaked at 25 m across all sampling sites (Fig. 5). Combined with depth-integrated gene abundances, *Sagittula castanea* was more abundant in the Equator region and the offshore than the BOB ( $p < 0.05$ ) (Fig. 6). *Trichodesmium*, UCYN-B, and  $\gamma$ -24774A11 were generally concentrated in the upper water

layers. For instance, *nifH* genes for *Trichodesmium* spp. reached up to  $3 \times 10^8$  copies  $L^{-1}$  in the surface water at Stn. I203 (Fig. 5). *Trichodesmium* and UCYN-B showed similar patterns regarding depth-integrated gene abundances, with higher gene copy numbers in the BOB and lower in the Equator region ( $p < 0.05$ ) (Fig. 6). For  $\gamma$ -24774A11, no significant differences were observed at different regions. In summary, our results demonstrated contrasting spatial patterns for *Trichodesmium* (higher at the BOB) and *Sagittula castanea* (higher in the Equator region and the offshore) in the EIO (Fig. 6).

### Statistical Analysis

Spatial distribution patterns (both horizontal and vertical) of the diazotrophic communities in the EIO are presented in Fig. 7. Horizontally, the surface samples from the same transect were almost grouped together (Fig. 7a), showing similar community structures in the same area. The surface samples in the BOB were mainly composed of Cyanophyceae, while samples in the Equator region and the offshore were mainly composed of Alphaproteobacteria (Fig. 7b). Vertically, we observed that the surface samples and the deeper samples were separated at 30% similarity (Fig. 7a). It indicated that the surface samples were distinct from other deeper samples, and the composition of the diazotrophic communities varied along the vertical gradient. From Fig. 7a, samples at 75 m and 200 m were almost grouped together except for samples from



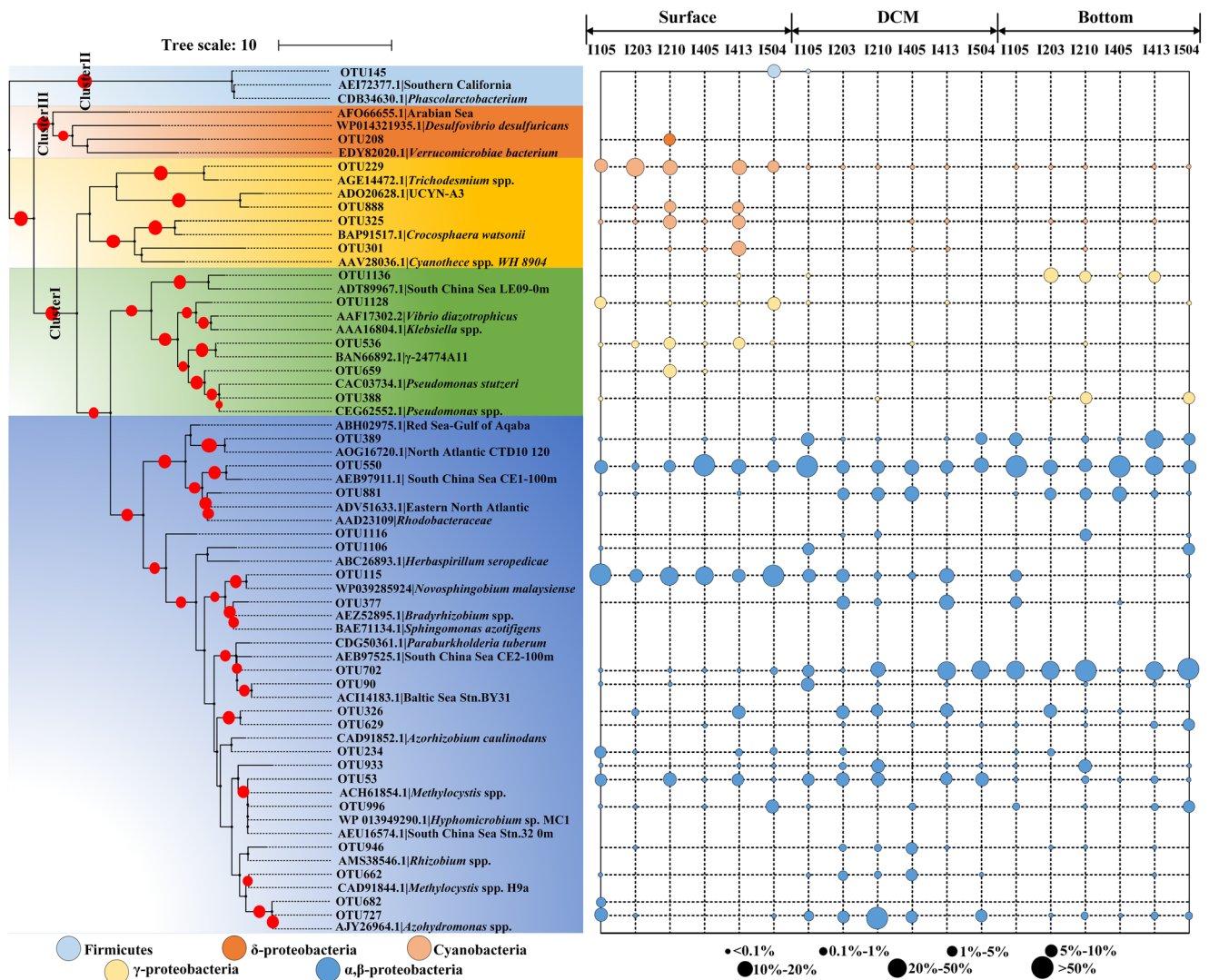


**Fig. 4** A neighbor-joining phylogenetic tree (left) and a bubble map to show OTU relative abundance (right) at each site. The tree was constructed by *nifH* gene amino acid sequences obtained from this study and reference sequences from GenBank. The topology of the tree was inferred

from 1000 bootstrap resampling, and bootstrap values greater than 50% were shown with red labels on branches. The bubble sizes corresponded to relative abundance of each OTU

Sta. I405. The two samples at Sta. I405 were mainly composed of Alphaproteobacteria. Whereas for other deeper samples, Betaproteobacteria was also an important component (Fig. 7b).

Correlations of the diazotrophic community and associated environmental factors were analyzed by CCA (Fig. 8). Temperature, salinity, phosphate, and ammonia were included in CCA after excluding environmental factors with VIFs > 20. The environmental factors in the first two axis explained > 83.63% of the total variance in the diazotrophic community distributions. Temperature ( $p = 0.001$ ), salinity ( $p = 0.001$ ), and phosphate ( $p = 0.001$ ) contributed significantly to the total variance and were closely associated with the first and second axes (999 times Monte Carlo permutations). The sample distributions in CCA were similar to NMDS which also presented

a vertical separation. Temperature positively correlated with the diazotrophic distributions in surface, while salinity and phosphate were driving distribution of the diazotrophic communities in deep water samples. Cyanobacteria were all positively correlated with temperature, while most of Proteobacteria were positively related to salinity and phosphate. Interestingly, we observed  $\gamma$ -24774A11 was plotted together with cyanobacteria, suggesting  $\gamma$ -24774A11 possibly shared same ecological niches with cyanobacteria.

The correlations between *nifH* gene abundances and various environmental parameters are listed in Table 5. Among which,  $\gamma$ -24774A11, *Trichodesmium*, and UCYN-B related *nifH* gene abundance were all exhibiting similar trends to the environmental parameters: significant negative correlations with water depth ( $p < 0.01$ ), salinity ( $p < 0.01$ ) and nutrients ( $p < 0.01$ ), and a

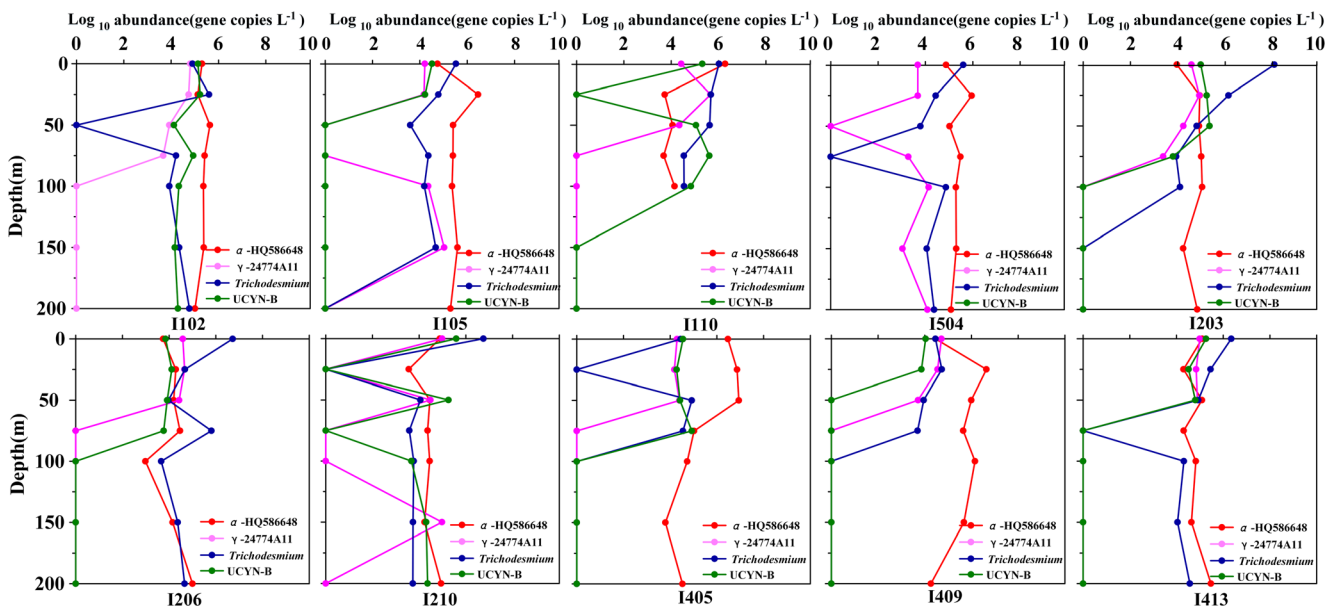


**Fig. 5** Depth profiles of *nifH* gene abundances ( $\log_{10}$  copies  $L^{-1}$ ) for *Sagittula castanea* (alpha-HQ586648),  $\gamma$ -24774A11, *Trichodesmium*, and UCYN-B. For convenience, one gene copy was used to represent where *nifH* genes were under detection

positive correlation with temperature ( $p < 0.01$ ). In contrast, *Sagittula castanea* was homogeneously distributed in the water column and therefore exhibited no correlation with depth and temperature, but showed significant negative correlations with nitrate and phosphate ( $p < 0.05$ ) (Table 5).

### Discussion

Recent studies have shown that putative  $N_2$ -fixing phylotypes of heterotrophic diazotrophs appeared to be ubiquitous in diverse marine and estuarine environments, even in deep, cold, or high-latitude waters where cyanobacteria were low or absent [61–64]. Due to their widespread distribution, heterotrophic diazotrophs are potentially important  $N_2$  fixers, and global N inputs solely based on cyanobacterial diazotrophs is likely underestimated. Similar to previous studies, our data elaborate that Proteobacteria are the most abundant diazotrophs in the EIO, especially in the equatorial region and deep waters. The prevalence of diverse heterotrophic  $N_2$ -fixing bacteria in oceans has been attributed to the overproduction of phytoplankton and accumulation of DOC in previous study [65].

During our cruise, we observed an unusually high phytoplankton primary productivity (Liu HJ et al. unpublished data) in the equatorial region which could be influenced by Wyrтки Jets [66]. The periodic Wyrтки Jets bring high-salinity and high-nutrient waters from 60° E to east along the equator [67]. Rahav et al. explained that addition of polysaccharide may increase efficiency of ectoenzymes such as  $\beta$ -glucosidase, and generated bioavailable molecules with enhanced polysaccharide hydrolysis [68]. Further, numerous studies have demonstrated that heterotrophic diazotrophs were stimulated by addition of nutrients or dissolved organic matter (DOM) [69, 70]. However, distribution of heterotrophic diazotrophs and their environmental drivers in marine ecosystems are still poorly understood. Further studies on biogeochemical, physio-ecological, and molecular aspects are needed to evaluate roles that heterotrophic diazotrophs play in nutrient and carbon cycling in global oceans.

Alphaproteobacterial genes were contributing the biggest fraction to the *nifH* gene diversity in our study, although previous studies have revealed that Gammaproteobacteria dominated global oceans [11, 16]. The dominance of Alphaproteobacteria and Betaproteobacteria in the

**Table 4** Sensitivity and accuracy of the standard curves determined by primer pairs and probes for different targets

Targets	Sensitivity				Accuracy test (copy no.)	
	Slope	$R^2$	Y-intercept	Linearity range	Added	Detected
<i>Trichodesmium</i> spp.	-3.225	0.996	39.987	$10^1$ – $10^7$	1000	958
UCYN-B	-3.192	0.997	37.381	$10^1$ – $10^7$	1000	1005
<i>Sagittula castanea</i>	-3.333	0.997	38.336	$10^1$ – $10^7$	1000	977
$\gamma$ -24774A11	-3.333	0.997	40.666	$10^1$ – $10^7$	1000	1027

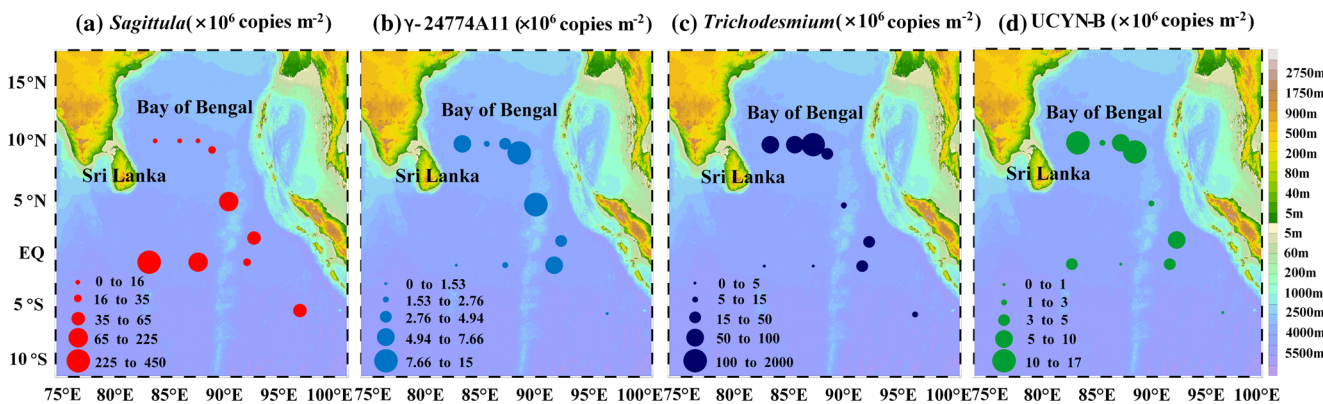


**Fig. 6** Depth-integrated (0–200 m) gene abundances ( $\times 10^6$  copies  $m^{-2}$ ) for *Sagittula castanea*,  $\gamma$ -24774A11, *Trichodesmium*, and UCYN-B in the EIO. Bubble sizes corresponded to gene abundances at each sampling station

diazotrophic communities was also reported in the Arabian Sea and the Western Equatorial region during northeast monsoon [14]. In the present study, OTU550 was the most abundant Alphaproteobacteria, as well as the dominant diazotroph in the EIO. The representative sequence of OTU550 shared 100% similarity with a new species named *Sagittula castanea* which was isolated from the oxygen minimum zone off Peru in the eastern tropical South Pacific (ETSP) [60]. *Sagittula castanea* has been confirmed capable of fixing  $N_2$  in the laboratory experiments, while it is still uncertain if this species is actively fixing  $N_2$  in natural environments [60]. In fact, *Sagittula*-related *nifH* sequences have been reported dominant in both shelf and open oceans of the ETSP, surface waters in the Indian Ocean, and the deep waters at the South China Sea, where  $N_2$  fixation was measurable [14, 51]. Presumably, non-cyanobacterial diazotrophs were responsible for  $N_2$  fixation in these regions. *Sagittula castanea* was recognized as a particle-attached lifestyle based on metabolic pathway analysis [60].

High C:N ratio contained in the particles provides sufficient organic carbon to heterotrophic diazotrophs. Due to *Sagittula castanea* was universally distributed in the euphotic zone (Figs. 4 and 5), this species exhibited no correlations with water depth, temperature, or salinity (Table 5). However, the negative correlations between *Sagittula castanea* and nitrate/phosphate revealed that the growth of *Sagittula castanea* might be limited by other factors rather than nutrients (Table 5).

In this study, a typical Gammaproteobacteria species with a broad geographic distribution,  $\gamma$ -24774A11, was also retrieved. Our qPCR results showed that the depth-integrated gene abundance of  $\gamma$ -24774A11 was two or three orders of magnitude lower than that of *Sagittula castanea* and *Trichodesmium* spp. (Fig. 6). Though  $\gamma$ -24774A11 was not dominant diazotroph in our study, its abundance was still comparable to other studies in global oceans [14, 16].  $\gamma$ -24774A11 always occurred in upper layers of the water

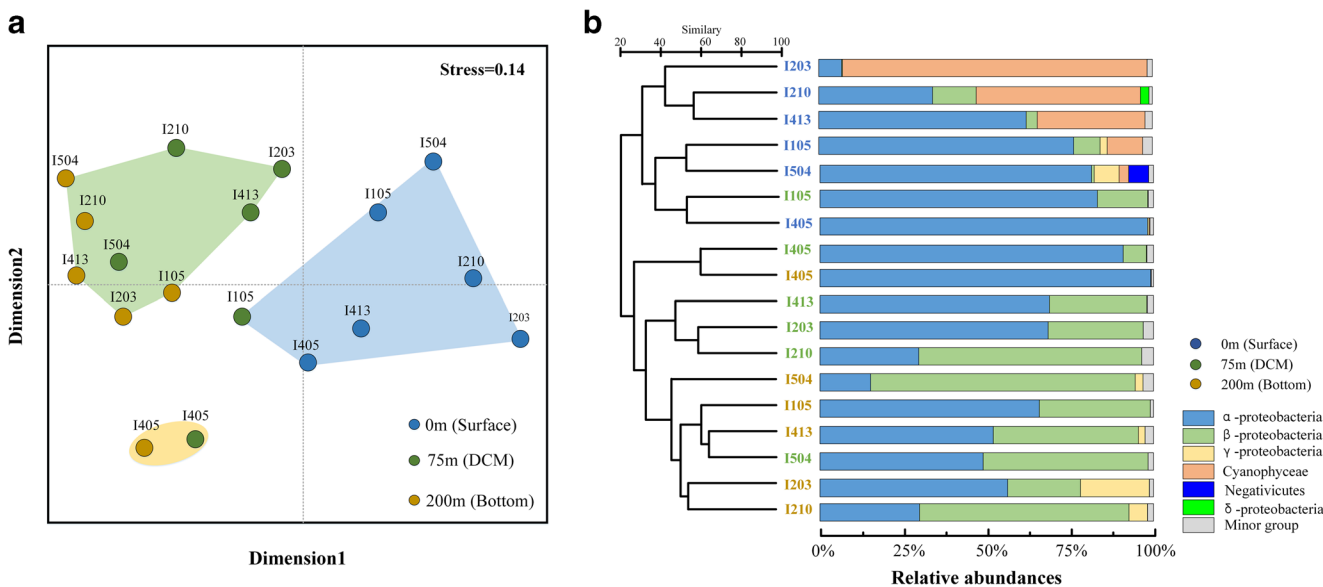


**Fig. 7** Non-metric multidimensional scaling (NMDS) analysis of diazotrophic communities (stress = 0.14, similarity = 30%) from the EIO (a) and corresponding community structures at class level (b). Different classes and samples from different depths were color coded

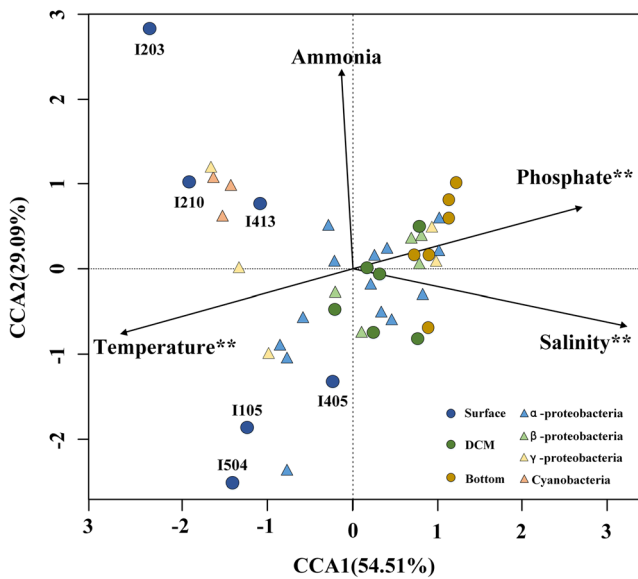


**Fig. 8** Canonical correspondence analysis (CCA) based on diazotrophic composition and biotic/abiotic parameters as explanatory variables. The two CCA axes (CCA1 and CCA2) explained 83.63% of total variations in abundance data. Arrows represented environmental parameters. Different colors of circle and triangle symbols represented different samples and taxa, respectively. Only the top 30 OTUs were included. Significance (\*\*) was determined by 999 Monte Carlo permutation tests with R V.3.0 software

column and became undetected below approximately 100 m (Fig. 5). The correlation analysis showed that  $\gamma$ -24774A11 abundances were controlled by depth and dissolved inorganic nitrogen (Table 5), which agreed well with a previous study conducted in the South Pacific Ocean [15]. Interestingly, we observed that the distribution of depth-integrated gene abundances of  $\gamma$ -24774A11 was similar to *Trichodesmium* and UCYN-B, but in contrast to *Sagittula castanea*. Our CCA also demonstrated the concurrent ecological niches between  $\gamma$ -24774A11 and cyanobacteria. As stated above, availability of DOC can be a limiting factor for the growth of heterotrophic  $N_2$ -fixing bacteria, and therefore, a positive correlation was expected between phytoplankton production and the abundance of  $\gamma$ -24774A11. However, in this study,  $\gamma$ -24774A11 had a negative correlation with Chl *a*. The same observation was also reported by Moisander et al. (2014), who suggested that environmental conditions in favor of

*Trichodesmium* and *Crocospaera watsonii* would benefit growth of  $\gamma$ -24774A11 [15].

Higher abundance of *Trichodesmium* spp. were found at BOB than the Equator region and the transect parallel to the coastline of the Sumatra, although hydrological conditions seemed favorable for *Trichodesmium* in the whole study area. Especially at Sta. I203, *Trichodesmium nifH* genes was up to  $1.5 \times 10^8$  *nifH* gene copies  $L^{-1}$  at the surface water according to the result of qPCR (Fig. 5). It was hard to explain the difference of *Trichodesmium* distribution in such similar hydrological conditions across the study area. Many studies have revealed that iron (Fe) is an important cofactor for nitrogenase, and it plays a crucial role in synthesis and expression of nitrogenase in diazotrophs [14, 30]. According to literature, dissolved Fe (dFe) in surface waters ranged from 0.1–0.62 nM in the north-eastern Indian Ocean, and the concentration decreased dramatically from the BOB to the Equator region [71, 72]. It was hypothesized that Fe availability might limit growth of *Trichodesmium* in the Equator regions, while Fe was not a limiting factor in the BOB. The similar result was also reported by Shiozaki et al. (2014), who observed high Fe concentration coupled with high abundance of *Trichodesmium* in the AS, while severely limited Fe concentration coupled with undetectable *Trichodesmium* in the Equator region [14]. Another possible explanation was meso-scale eddy circulations frequently occurred in the BOB during pre-southwest monsoon. Anti-cyclonic (warm-core) eddies are a common phenomenon in the Indian Ocean during pre-southwest monsoon, and they could influence the distribution of phytoplankton via regulating vertical environmental parameters [73]. Jyothibabu reported that most *Trichodesmium* blooms recorded in the Indian Ocean were during the pre-southwest monsoon, and warm-core eddies caused downwelling of the surface waters and provided optimal growing conditions for *Trichodesmium* [74]. Furthermore, the specific gas vesicles in *Trichodesmium* could provide buoyancy and help them migrate vertically in water columns to obtain phosphate and other nutrients from deep waters, and help them float on the sea surface forming patches, bands, or mats depending upon the status of the sea [75].

Except for *Trichodesmium*, other cyanobacteria such as UCYN-A3, *Crocospaera watsonii*, and *Cyanothece* sp.

**Table 5** Correlation analysis of *nifH* gene abundances ( $\log_{10}$  copies  $L^{-1}$ ) (*Trichodesmium* spp., UCYN-B, *Sagittula castanea*, and  $\gamma$ -24774A11) and environmental parameters

Targets	Depth	<i>T</i>	Salinity	Chl <i>a</i>	$PO_4^{3-}$	$NH_4^+$	$NO_3^-$	$NO_2^-$
<i>Trichodesmium</i> spp.	-0.45**	0.433**	-0.506**	0.041	-0.434**	0.042	-0.411**	-0.037
UCYN-B	-0.325**	0.317**	-0.398**	-0.061	-0.335**	0.063	-0.196	-0.094
<i>Sagittula castanea</i>	-0.174	0.155	0.069	0.023	-0.259*	0.044	-0.286*	-0.104
$\gamma$ -24774A11	-0.622**	0.595**	-0.584**	-0.107	-0.620**	0.252*	-0.582**	-0.253*

\* $p < 0.05$ ; \*\* $p < 0.01$

WH 8904 were also retrieved in the present study via high throughput sequencing. UCYN-A were reported widely distributed in tropical and subtropical oceans and made significant contribution to BNF in these regions [76, 77]. According to *nifH* phylogeny, the UCYN-A lineage was divided into at least four main sublineages, namely, UCYN-A1, UCYN-A2, UCYN-A3, and UCYN-A4 [78]. However, in the present study, only UCYN-A3 was recovered via high throughput sequencing. Turk-Kubo et al. (2016) reported that the UCYN-A3 sublineage is more widely distributed in oligotrophic waters than other three sublineages [79]. It has been reported that optimum temperature for UCYN-A lineage was 24 °C, but water temperature in the present study ranged from 29.3 to 31.1 °C, which was not a favorable condition in general [31]. Therefore, water temperature and nutrient levels likely explained the low occurrence of UCYN-A in our study. In addition, *Crocospaera watsonii* was also presented low abundance in our study. Fu et al. (2014) reported that thermal limits for *Crocospaera watsonii* ranged from 24 to 32 °C, and the optimum growth temperatures was 30 °C [80]. Our correlation analysis also showed gene abundance of *Crocospaera watsonii* was positively related to water temperature and negatively related to salinity and phosphate. Though the temperature in the EIO seemed favorable for the growth of *Crocospaera watsonii*, it was still presented in low abundance. Shiozaki et al. [14] suggested that the shallower nitracline depths, which could result in higher upward fluxes of nutrients to the surface water, were responsible for the low abundance of UCYN-B in the EIO [52]. Until now, little is known about controlling factors that drive distributions of *Cyanothece* sp. WH8904.

Our results indicated that temperature, salinity, and phosphate were major environmental factors to explain variation and distribution of the diazotrophic community in the EIO. Similarly, it was reported in the northern South China Sea where salinity and phosphate were responsible for spatio-temporal variations of the diazotrophic communities [11]. Also, the diazotrophic communities may exhibit vertical distribution patterns along water depths; however, Loescher et al. (2014) suggested that water depth integrated temperature, salinity, and other physical variables, as they were all highly collinear with depth [70]. Nevertheless, distribution and composition of the diazotrophic communities were strongly influenced by these environmental variables. Ammonia was also included in our CCA analysis, in spite of its influence on the diazotrophic communities was not significant. In addition, due to highly collinearity with other factors, nitrate and nitrite were not included in our CCA analysis. But, this could not eliminate potential roles of such inorganic nutrients in structuring spatial heterogeneity in the diazotrophic communities. In fact, it is generally believed that reactive inorganic nutrient concentrations regulate the abundance of diazotrophs, as well as N<sub>2</sub> fixation [16]. Presumably, these widespread

heterotrophic diazotrophs may have many adaptive mechanisms to deal with high concentration of various inorganic nutrients. For instance, a recent comparative genomics study revealed that nitrogenase in an isolated heterotrophic bacterium can be activated with high ammonia concentration in lack of functional CbbP or DraT2 proteins [81]. Nevertheless, how heterotrophic diazotrophs respond to their ambient nutrients warrant future studies.

## Conclusion

To the best of our knowledge, this study presented the first evidence of composition and distribution of the diazotrophic communities in the EIO during the pre-southwest monsoon. Due to logistical constraints, our results were all generated from molecular data, and direct cell counts were not included in our study. Also due to possibly low abundance of diazotrophs, we applied high numbers of PCR cycles in gene amplification. Although it has been a well-developed protocol [e.g., 59], we realized that high PCR cycles might generate PCR bias and skew community structure characterization. In addition, primers used in our nested PCR were recently reported containing one mismatch that might influence the results of high throughput sequencing [64]. Despite these challenges, we observed diverse groups of diazotrophs that belong to Alpha-, Beta-, Gamma-proteobacterial groups; cyanobacterial cluster; and Firmicutes. Among which, Proteobacteria was the most dominant diazotroph in the EIO during pre-southwest monsoon, potentially contributing significantly to BNF in this oligotrophic ecosystem. Our results were in good agreement with previous studies conducted in the Western Indian Ocean, where heterotrophic bacteria were also reported dominant within the euphotic zone. Up to date, it is still poorly understood about ecology of marine heterotrophic diazotrophs and their actual contribution to BNF in the EIO. Further investigations on niche specialization and eco-physiological characterization of diazotrophs are greatly needed in order to better understand interactions of heterotrophic and cyanobacterial diazotrophs and how these interactions influence global nitrogen cycling.

**Acknowledgements** We thank Prof. Dongxiao Wang from South China Sea Institute of Oceanology, Chinese Academy of Sciences for providing hydrographic (CTD) data. Dr. Liangliang Kong at McGill University and Dr. Xiaomin Xia at the Hong Kong University of Science and Technology are also acknowledged for their help and technical support during experiments. We also gratefully acknowledge the crew of R/V “Shiyan 3” and all participants for their assistance during the cruise.

**Author Contributions** This work was designed by JS. Samples were collected by CW, HL, and XW. CW performed experiments and analyzed data. CG performed the nutrients analysis. CW drafted the paper and revised by JK and PL. All authors contributed to the writing of the manuscript.

**Funding Information** This study was supported by the National Natural Science Foundation of China (41876134, 41276124, and 41676112) and NSFC open research cruises (NORC2017-10), the Science Fund for University Creative Research Groups in Tianjin (TD12-5003), the Changjiang Scholar Program of Chinese Ministry of Education to JS, and endowment support from Stroud Water Research Center to JK.

## References

- Dugdale RC, Goering JJ (1967) Uptake of new and regenerated forms of nitrogen in primary productivity. *Limnol Oceanogr* 12: 196–206. <https://doi.org/10.4319/lo.1967.12.2.0196>
- Zehr JP (2011) Nitrogen fixation by marine cyanobacteria. *Trends Microbiol* 19:162–173. <https://doi.org/10.1016/j.tim.2010.12.004>
- Gradoville MR, Bombar D, Crump BC, Letelier RM, Zehr JP, White AE (2017) Diversity and activity of nitrogen-fixing communities across ocean basins. *Limnol Oceanogr* 62:1895–1909. <https://doi.org/10.1002/lno.10542>
- Levitan O, Rosenberg G, Setlik I et al (2007) Elevated CO<sub>2</sub> enhances nitrogen fixation and growth in the marine cyanobacterium *Trichodesmium*. *Glob Chang Biol* 13:531–538. <https://doi.org/10.1111/j.1365-2486.2006.01314.x>
- Benavides M, Voss M (2015) Five decades of N<sub>2</sub> fixation research in the North Atlantic Ocean. *Front Mar Sci* 2:1–40. <https://doi.org/10.3389/fmars.2015.00040>
- Yang L, Wang DX, Huang J, Wang X, Zeng L, Shi R, He Y, Xie Q, Wang S, Chen R, Yuan J, Wang Q, Chen J, Zu T, Li J, Sui D, Peng S (2015) Toward a mesoscale hydrological and marine meteorological observation network in the South China Sea. *Bull Am Meteorol Soc* 96(7):1117–1135. <https://doi.org/10.1175/BAMS-D-14-00159.1>
- Carpenter EJ, Subramaniam A, Capone DG (2004) Biomass and primary productivity of the cyanobacterium *Trichodesmium* spp. in the tropical N Atlantic Ocean. *Deep-Sea Res I* 51:173–203. <https://doi.org/10.1016/j.dsr.2003.10.006>
- Sohm JA, Webb EA, Capone DG (2011) Emerging patterns of marine nitrogen fixation. *Nat Rev Microbiol* 9(7):499–508. <https://doi.org/10.1038/nrmicro2594>
- Zehr JP, Jenkins BD, Short SM, Steward GF (2003) Nitrogenase gene diversity and microbial community structure: a cross-system comparison. *Environ Microbiol* 5:539–554. <https://doi.org/10.1046/j.1462-2920.2003.00451.x>
- Zehr JP, Mellon MT, Zani S (1998) New nitrogen-fixing microorganisms detected in oligotrophic oceans by amplification of nitrogenase (*nifH*) genes. *Appl Environ Microbiol* 64:3444–3450
- Kong LL, Jing HM, Kataoka T, Sun J, Liu H (2011) Phylogenetic diversity and spatio-temporal distribution of nitrogenase genes (*nifH*) in the northern South China Sea. *Aquat Microb Ecol* 65(1): 15–27. <https://doi.org/10.3354/ame01531>
- Monteiro FM, Follows MJ, Dutkiewicz S (2010) Distribution of diverse nitrogen fixers in the global ocean. *Glob Biogeochem Cycles* 24:GB3017. <https://doi.org/10.1029/2009GB003731>
- Cheung SY, Suzuki K, Saito H, Umezawa Y, Xia X, Liu H (2017) Highly heterogeneous diazotroph communities in the Kuroshio current and the Tokara Strait, Japan. *PLoS One* 12(10):e0186875. <https://doi.org/10.1371/journal.pone.0186875>
- Shiozaki T, Ijichi M, Kodama T, Takeda S, Furuya K (2014) Heterotrophic bacteria as major nitrogen fixers in the euphotic zone of the Indian Ocean. *Glob Biogeochem Cycles* 28:1096–1110. <https://doi.org/10.1002/2014GB004886>
- Moisander PH, Serros T, Paerl RW, Beinart RA, Zehr JP (2014) Gammaproteobacterial diazotrophs and *nifH* gene expression in surface waters of the South Pacific Ocean. *ISME J* 8(10):1962–1973. <https://doi.org/10.1038/ismej.2014.49>
- Bombar D, Paerl RW, Riemann L (2016) Marine non-cyanobacterial diazotrophs: moving beyond molecular detection. *Trends Microbiol* 24(11):916–927. <https://doi.org/10.1016/j.tim.2016.07.002>
- Schott FA, Xie SP, McCreary JP (2009) Indian ocean circulation and climate variability. *Rev Geophys* 47(1):RG1002. <https://doi.org/10.1029/2007RG000245>
- Wang J, Kan JJ, Zhang XD et al (2017) Archaea dominate the ammonia-oxidizing community in deep-sea sediments of the Eastern Indian Ocean—from the equator to the Bay of Bengal. *Front Microbiol* 8:1–16. <https://doi.org/10.3389/fmicb.2017.00415>
- Singh A, Jani RA, Ramesh R (2010) Spatiotemporal variations of the  $\delta^{18}\text{O}$ -salinity relation in the northern Indian Ocean. *Deep-Sea Res I* 57(11):1422–1431. <https://doi.org/10.1016/j.dsr.2010.08.002>
- Singh A, Ramesh R (2015) Environmental controls on new and primary production in the northern Indian Ocean. *Prog Oceanogr* 131(3):138–145. <https://doi.org/10.1016/j.pocean.2014.12.006>
- Lévy M, Shankar D, André JM, Shenoi SSC, Durand F, de Boyer Montégut C (2009) Basin-wide seasonal evolution of the Indian Ocean's phytoplankton blooms. *J Geophys Res Oceans* 112: C12014. <https://doi.org/10.1029/2007JC004090>
- Gomes HR, Goes JI, Saino T (2000) Influence of physical processes and freshwater discharge on the seasonality of phytoplankton regime in the Bay of Bengal. *Cont Shelf Res* 20:313–330. [https://doi.org/10.1016/S0278-4343\(99\)00072-2](https://doi.org/10.1016/S0278-4343(99)00072-2)
- Kumar SP, Muraleedharan PM, Prasad TG et al (2002) Why is the Bay of Bengal less productive during summer monsoon compared to the Arabian Sea? *Geophys Res Lett* 29(24):2235–3770. <https://doi.org/10.1002/2016JC012639>
- Madhupratap M, Gauns M, Ramaiah N et al (2003) Biogeochemistry of the Bay of Bengal: physical, chemical and primary productivity characteristics of the central and western Bay of Bengal during summer monsoon. *Deep-Sea Res II* 50(5): 881–896. [https://doi.org/10.1016/S0967-0645\(02\)00611-2](https://doi.org/10.1016/S0967-0645(02)00611-2)
- Hegde S, Anil AC, Patil JS et al (2008) Influence of environmental settings on the prevalence of *Trichodesmium* spp. in the Bay of Bengal. *Mar Ecol Prog Ser* 356(01):93–101. <https://doi.org/10.3354/meps07259>
- Gandhi N, Singh A, Prakash S, Ramesh R, Raman M, Sheshshayee MS, Shetye S (2011) First direct measurements of N<sub>2</sub> fixation during a *Trichodesmium* bloom in the eastern Arabian Sea. *Glob Biogeochem Cycles* 25:GB4014. <https://doi.org/10.1029/2010GB003970>
- Ahmed A, Gauns M, Kurian S (2017) Nitrogen fixation rates in the eastern Arabian Sea. *Estuar Coast Shelf Sci* 191:74–83. <https://doi.org/10.1016/j.ecss.2017.04.005>
- Bird C, Wyman M (2012) Transcriptionally active heterotrophic diazotrophs are widespread in the upper water column of the Arabian Sea. *FEMS Microbiol Ecol* 84(1):189–200. <https://doi.org/10.1111/1574-6941.12049>
- Kitajima S, Furuya K, Hashihama F, Takeda S, Kanda J (2009) Latitudinal distribution of diazotrophs and their nitrogen fixation in the tropical and subtropical western North Pacific. *Limnol Oceanogr* 54(2):537–547. <https://doi.org/10.4319/lo.2009.54.2.0537>
- Shiozaki T, Bombar D, Riemann L, Hashihama F, Takeda S, Yamaguchi T, Ehama M, Hamasaki K, Furuya K (2017) Basin scale variability of active diazotrophs and nitrogen fixation in the North Pacific, from the tropics to the subarctic Bering Sea. *Glob Biogeochem Cycles* 31(6):996–1009. <https://doi.org/10.1002/2017GB005681>
- Church MJ, Mahaffey C, Letelier RM, Lukas R, Zehr JP, Karl DM (2009) Physical forcing of nitrogen fixation and diazotroph community structure in the North Pacific subtropical gyre. *Glob Biogeochem Cycles* 23:GB2020. <https://doi.org/10.1029/2008GB003418>

32. Benavides M, Moisaner PH, Daley MC, Bode A, Aristegui J (2016) Longitudinal variability of diazotroph abundances in the subtropical North Atlantic Ocean. *J Plankton Res* 38(3):662–672. <https://doi.org/10.1093/plankt/fbv121>
33. Goebel NL, Turk KA, Achilles KM, Paerl R, Hewson I, Morrison AE, Montoya JP, Edwards CA, Zehr JP (2010) Abundance and distribution of major groups of diazotrophic cyanobacteria and their potential contribution to N<sub>2</sub> fixation in the tropical Atlantic Ocean. *Environ Microbiol* 12(12):3272–3289. <https://doi.org/10.1111/j.1462-2920.2010.02303.x>
34. Shiozaki T, Nagata T, Ijichi M (2015) Nitrogen fixation and the diazotroph community in the temperate coastal region of the northwestern North Pacific. *Biogeosciences* 12:4751–4764. <https://doi.org/10.5194/bg-12-4751-2015>
35. Foster RA, Subramaniam A, Mahaffey C (2007) Influence of the Amazon River plume on distributions of free-living and symbiotic cyanobacteria in the western tropical North Atlantic Ocean. *Limnol Oceanogr* 52(2):517–532. <https://doi.org/10.4319/lo.2007.52.2.0517>
36. Grasshoff K, Ehrhardt M, Kremling K (1982) *Methods of seawater analysis*. ISBN (Verlag Chemie), 3–527, 25,998–26,008
37. Schmidt TM, Delong EF, Pace NR (1991) Analysis of a marine picoplankton community by 16S rRNA gene cloning and sequencing. *J Bacteriol* 173:4371–4378. <https://doi.org/10.1128/jb.173.14.4371-4378.1991>
38. Kan JJ, Clingenpeel S, Macur RE et al (2011) Archaea in Yellowstone Lake. *ISME J* 5(11):1784–1795. <https://doi.org/10.1038/ismej.2011.56>
39. Zhang Y, Yang Q, Ling J et al (2017) Diversity and structure of diazotrophic communities in mangrove rhizosphere, revealed by high-throughput sequencing. *Front Microbiol* 8(2032). <https://doi.org/10.3389/fmicb.2017.02032>
40. Caporaso JG, Kuczynski J, Stombaugh J, Bittinger K, Bushman FD, Costello EK, Fierer N, Peña AG, Goodrich JK, Gordon JL, Huttley GA, Kelley ST, Knights D, Koenig JE, Ley RE, Lozupone CA, McDonald D, Muegge BD, Pirrung M, Reeder J, Sevinsky JR, Turnbaugh PJ, Walters WA, Widmann J, Yatsunenko T, Zaneveld J, Knight R (2010) QIIME allows analysis of high-throughput community sequencing data. *Nat Methods* 7(5):335–336. <https://doi.org/10.1038/nmeth.f.303>
41. Magoč T, Salzberg SL (2010) FLASH: fast length adjustment of short reads to improve genome assemblies. *Bioinformatics* 27(21):2957–2963. <https://doi.org/10.1093/bioinformatics/btr507>
42. Bolger AM, Lohse M, Usadel B (2014) Trimmomatic: a flexible trimmer for Illumina sequence data. *Bioinformatics* 30(15):2114–2120. <https://doi.org/10.1093/bioinformatics/btu170>
43. Kunin V, Engelbrekton A, Ochman H, Hugenholtz P (2010) Wrinkles in the rare biosphere: pyrosequencing errors can lead to artificial inflation of diversity estimates. *Environ Microbiol* 12:118–123. <https://doi.org/10.1111/j.1462-2920.2009.02051.x>
44. Huse SM, Huber JA, Morrison HG, Sogin ML, Welch DM (2007) Accuracy and quality of massively parallel DNA pyrosequencing. *Genome Biol* 8:R143. <https://doi.org/10.1186/gb-2007-8-7-r143>
45. Edgar RC, Haas BJ, Clemente JC, Quince C, Knight R (2011) UCHIME improves sensitivity and speed of chimera detection. *Bioinformatics* 27(16):2194–2200. <https://doi.org/10.1093/bioinformatics/btr381>
46. Edgar RC (2010) Search and clustering orders of magnitude faster than BLAST. *Bioinformatics* 26(19):2460–2461. <https://doi.org/10.1093/bioinformatics/btq461>
47. Altschul SF, Madden TL, Schäffer AA et al (1997) Gapped BLAST and PSI-BLAST: a new generation of protein database search programs. *Nucleic Acids Res* 25:3389–3402. <https://doi.org/10.1093/nar/25.17.3389>
48. Huson DH, Auch AF, Qi J, Schuster SC (2007) MEGAN analysis of metagenomic data. *Genome Res* 17(3):377–386. <https://doi.org/10.1101/gr.5969107>
49. Kumar S, Stecher G, Tamura K (2016) MEGA7: molecular evolutionary genetics analysis version 7.0 for bigger datasets. *Mol Biol Evol* 33:1870–1874. <https://doi.org/10.1093/molbev/msw054>
50. Letunic I, Bork P (2011) Interactive tree of life v2: online annotation and display of phylogenetic trees made easy. *Nucleic Acids Res* 39:475–478. <https://doi.org/10.1093/nar/gkr201>
51. Zhang Y, Zhao ZH, Sun J (2011) Diversity and distribution of diazotrophic communities in the South China Sea deep basin with mesoscale cyclonic eddy perturbations. *FEMS Microbiol Ecol* 78(3):417–427. <https://doi.org/10.1111/j.1574-6941.2011.01174.x>
52. R Development Core Team (2008) R: a language and environment for statistical computing. R Foundation for Statistical Computing, Vienna, Austria. ISBN 3–900051–07–0, URL <http://www.R-project.org>. Accessed 31 Oct 2016
53. Chao A, Jost L (2012) Coverage-based rarefaction and extrapolation: standardizing samples by completeness rather than size. *Ecology* 93:2533–2547. <https://doi.org/10.1890/11-1952.1>
54. Hsieh TC, Ma KH, Chao A (2016) iNEXT: an R package for rarefaction and extrapolation of species diversity (hill numbers). *Methods Ecol Evol* 7:1451–1456. <https://doi.org/10.1111/2041-210X.12613>
55. Clarke KR, Gorley RN (2006) *PRIMER v6: user manual/tutorial*. Marine Laboratory, Plymouth, UK, pp 190
56. ter Braak CJE, Šmilauer P (2002) *Canoco for Windows*, version 4.5. Biometris-Plant Research International, Wageningen
57. Lepš J, Šmilauer P (2003) *Multivariate analysis of ecological data using CANOCO*. Cambridge University Press, Cambridge
58. Dixon P (2003) VEGAN, a package of R functions for community ecology. *J Veg Sci* 14(6):927–930. <https://doi.org/10.1111/j.1654-1103.2003.tb02228.x>
59. Schlitzer R (2018) Ocean data view. <https://odv.awi.de>. Accessed 19 May 2018
60. Martínez-Pérez C, Mohr W, Schwedt A, Dürschlag J, Callbeck CM, Schunck H, Dekaezemaeker J, Buckner CRT, Lavik G, Fuchs BM, Kuypers MMM (2018) Metabolic versatility of a novel N<sub>2</sub>-fixing Alphaproteobacterium isolated from a marine oxygen minimum zone. *Environ Microbiol* 20(2):755–768. <https://doi.org/10.1111/1462-2920.14008>
61. Riemann L, Farnelid H, Steward GF (2010) Nitrogenase genes in non-cyanobacterial plankton: prevalence, diversity and regulation in marine waters. *Aquat Microb Ecol* 61:235–247. <https://doi.org/10.3354/ame01431>
62. Farnelid H, Andersson AF, Bertilsson S, al-Soud WA, Hansen LH, Sørensen S, Steward GF, Hagström Å, Riemann L (2011) Nitrogenase gene amplicons from global marine surface waters are dominated by genes of non-cyanobacteria. *PLoS One* 6(4):e19223. <https://doi.org/10.1371/journal.pone.0019223>
63. Bentzon-Tilia M, Traving SJ, Mantiki M, Knudsen-Leerbeck H, Hansen JLS, Markager S, Riemann L (2015) Significant N<sub>2</sub> fixation by heterotrophs, photoheterotrophs and heterocystous cyanobacteria in two temperate estuaries. *ISME J* 9(2):273–285. <https://doi.org/10.1038/ismej.2014.119>
64. Delmont TO, Quince C, Shaiber A et al (2018) Nitrogen-fixing populations of Planctomycetes and Proteobacteria are abundant in surface ocean metagenomes. *Nat Microbiol* 3:804–813. <https://doi.org/10.1038/s41564-018-0176-9>
65. Halm H, Lam P, Ferdelman TG, Lavik G, Dittmar T, LaRoche J, D'Hondt S, Kuypers MMM (2012) Heterotrophic organisms dominate nitrogen fixation in the South Pacific Gyre. *ISME J* 6(6):1238–1249. <https://doi.org/10.1038/ismej.2011.182>
66. Duan YL, Liu L, Han G, Liu H, Yu W, Yang G, Wang H, Wang H, Liu Y, Zahid, Waheed H (2016) Anomalous behaviors of Wyrkt

- Jets in the equatorial Indian Ocean during 2013. *Sci Rep* 6:29688. <https://doi.org/10.1038/srep29688>
67. Qian G, Wang J, Kan JJ, Zhang X, Xia Z, Zhang X, Miao Y, Sun J (2018) Diversity and distribution of anammox bacteria in water column and sediments of the Eastern Indian Ocean. *Int Biodeterior Biodegrad* 133:52–62. <https://doi.org/10.1016/j.ibiod.2018.05.015>
  68. Rahav E, Giannetto MJ, Bar-Zeev (2016) Contribution of mono and polysaccharides to heterotrophic N<sub>2</sub> fixation at the eastern Mediterranean coastline. *Sci Rep* 6:27858. <https://doi.org/10.1038/srep27858>
  69. Moisander PH, Zhang RF, Boyle EA, Hewson I, Montoya JP, Zehr JP (2012) Analogous nutrient limitations in unicellular diazotrophs and *Prochlorococcus* in the South Pacific Ocean. *ISME J* 6:733–744. <https://doi.org/10.1038/ismej.2011.152>
  70. Loescher CR, Großkopf T, Desai FD et al (2014) Facets of diazotroph in the oxygen minimum zone waters off Peru. *ISME J* 8(11):2180–2192. <https://doi.org/10.1038/ismej.2014.71>
  71. Grand MM, Measures CI, Hatta M, Hiscock WT, Buck CS, Landing WM (2015) Dust deposition in the eastern Indian Ocean: the ocean perspective from Antarctica to the Bay of Bengal. *Glob Biogeochem Cycles* 29(3):357–374. <https://doi.org/10.1002/2014GB004898>
  72. Grand MM, Measures CI, Hatta M, Hiscock WT, Landing WM, Morton PL, Buck CS, Barrett PM, Resing JA (2015) Dissolved Fe and Al in the upper 1000 m of the eastern Indian Ocean: a high-resolution transect from the Antarctic margin to the bay of Bengal. *Glob Biogeochem Cycles* 29(3):375–396. <https://doi.org/10.1002/2014GB004920>
  73. He Q, Zhan H, Shuai Y (2017) Phytoplankton bloom triggered by an anticyclonic eddy: the combined effect of eddy-Ekman pumping and winter mixing. *J Geophys Res-Oceans* 122:4886–4901. <https://doi.org/10.1002/2017JC012763>
  74. Jyothibabu R, Karnan C, Jagadeesan L, Arunpandi N, Pandiarajan RS, Muraleedharan KR, Balachandran KK (2017) *Trichodesmium* blooms and warm-core ocean surface features in the Arabian Sea and the Bay of Bengal. *Mar Pollut Bull* 121(1–2):201–215. <https://doi.org/10.1016/j.marpolbul.2017.06.002>
  75. Wu C, Fu FX, Sun J et al (2018) Nitrogen fixation by *Trichodesmium* and unicellular diazotrophs in the northern South China Sea and the Kuroshio in summer. *Sci Rep* 8(2415). <https://doi.org/10.1038/s41598-018-20743-0>
  76. Cabello AM, Cornejo-Castillo FM, Raho N, Blasco D, Vidal M, Audic S, de Vargas C, Latasa M, Acinas SG, Massana R (2016) Global distribution and vertical patterns of a prymnesiophyte–cyanobacteria obligate symbiosis. *ISME J* 10(3):693–706. <https://doi.org/10.1038/ismej.2015.147>
  77. Stenegren M, Caputo A, Berg C, Bonnet S, Foster RA (2018) Distribution and drivers of symbiotic and free-living diazotrophic cyanobacteria in the Western Tropical South Pacific. *Biogeosciences* 15(5):1559–1578. <https://doi.org/10.5194/bg-15-1559-2018>
  78. Cornejo-Castillo FM, Cabello AM, Salazar G, Sánchez-Baracaldo P, Lima-Mendez G, Hingamp P, Alberti A, Sunagawa S, Bork P, de Vargas C, Raes J, Bowler C, Wincker P, Zehr JP, Gasol JM, Massana R, Acinas SG (2016) Cyanobacterial symbionts diverged in the late cretaceous towards lineage-specific nitrogen fixation factories in single-celled phytoplankton. *Nat Commun* 7:11071. <https://doi.org/10.1038/ncomms11071>
  79. Turk-Kubo KA, Farnelid HM, Shilova IN, Henke B, Zehr JP (2016) Distinct ecological niches of marine symbiotic N<sub>2</sub>-fixing cyanobacterium *Candidatus atelocyanobacterium thalassa* sublineages. *J Phycol* 53(2):451–461. <https://doi.org/10.1111/jpy.12505>
  80. Fu FX, Yu E, Garcia NS, Gale J, Luo Y, Webb EA, Hutchins DA (2014) Differing responses of marine N<sub>2</sub>-fixers to warming and consequences for future diazotroph community structure. *Aquat Microb Ecol* 72:33–46. <https://doi.org/10.3354/ame01683>
  81. Heiniger EK, Oda Y, Samanta SK, Harwood CS (2012) How post-translational modification of nitrogenase is circumvented in *Rhodospseudomonas palustris* strains that produce hydrogen gas constitutively. *Appl Environ Microbiol* 78:1023–1032. <https://doi.org/10.1128/AEM.07254-11>